Self-presentation

I.   **Name and surname:**   Dorota Kowalska

II.   **Diplomas obtained, academic/artistic degrees – including the name, place and year of issue, and the title of doctoral thesis**

- M.Sc. in Physics in the subject of earth and atmosphere physics,
Adam Mickiewicz University, Poznan, Faculty of Physics, 1999
"Dynamics of deactivation of benzopyranthione and its derivatives in the triplet state"

- Ph.D. in Physics,
Adam Mickiewicz University, Poznan, Faculty of Physics, 2006
"Spectral and photophysical properties of selected polyatomic molecules in higher excited states"

III.   **Information about employment in scientific/artistic institutions**

2006/08 – 2008/05	postdoctoral fellow Department of Chemistry/ Laser Chemistry Group University of Saskatchewan, Saskatoon, Canada
2008/06 – 2009/05	scholarship *"Beca de Investigacion CajaCanarias"* Universidad de La Laguna, Tenerife, Spain
2009/11 – 2010/10	scholarship *"Beca de Investigacion CajaCanarias"* Universidad de La Laguna, Tenerife, Spain
2011/10 – 2014/12	postdoctoral fellow Institute of Physics, Nicolaus Copernicus University, Toruń, Poland
2015/02 – up to date	postdoctoral fellow Institute of Physics, Nicolaus Copernicus University, Toruń, Poland

IV.   **Indication of achievement* resulting from article 16 item 2 of the Act of Law dated to 14th of March 2003 on academic degrees and academic title as well as on degrees and title in the field of art (Official Journal, 2016, item 882 with later amendments):**

a) **Title of the scientific/artistic achievement**

„Silver nanowires as structures enhancing the optical response of photosynthetic proteins"

The scientific achievement is described in 5 publications listed below in the subsection IV.b

b) (author/authors, title/titles of publication, year of issue, publisher)

[H1] M. Olejnik, B. Krajnik, <u>D. Kowalska</u>, M. Twardowska, N. Czechowski, E. Hofmann, S. Maćkowski,
"Imaging of fluorescence enhancement in photosynthetic complexes coupled to silver nanowires",
2013, Applied Physics Letters, 102, pages: 083703/1-083703/5, IF: 3,515

[H2] <u>D. Kowalska</u>, B. Krajnik, M. Olejnik, M. Twardowska, N. Czechowski, E. Hofmann, S. Maćkowski,
"Metal - enhanced fluorescence of chlorophylls in light-harvesting complexes coupled to silver nanowires",
2013, The Scientific World Journal, 2013, pages: 670412/1-670412/12, IF: 1,219

[H3] M. Szalkowski, K. Sulowska, J. Grzelak, J. Niedziółka-Jönsson, E. Rozniecka, <u>D. Kowalska</u>, S. Maćkowski,
"Wide-field fluorescence microscopy of real-time bioconjugation sensing",
2018, Sensors 18, 290, pages: 1-10, IF: 2,475

[H4] <u>D. Kowalska</u>, M. Szalkowski, K. Ashraf, J. Grzelak, H. Lokstein, J. Niedziolka-Jonsson, R. Cogdell, S. Maćkowski,
"Spectrally selective fluorescence imaging of Chlorobaculum tepidum reaction centers conjugated to chelator modified silver nanowires",
2018, Photosynthesis Research, 135, pages: 329-336, IF: 3,091

[H5] M. Szalkowski, J. Olmos, D. Buczyńska, S. Maćkowski, <u>D. Kowalska</u>, J. Kargul,
"Plasmon-induced absorption of blind chlorophylls in photosynthetic proteins assembled on silver nanowires",
2017, Nanoscale, 9, pages: 10475-10486, IF: 7,233

c) Description of scientific/artistic objectives of the above work/works and accomplished results, including description of their potential use.

1. Introduction

The global annual energy demand, according to the International Energy Agency, is 15 TW [1]. On a cloudless day, on average, every square meter of the Earth's surface is exposed for one hour to sunlight of about 1 kW [2]. This means that the amount of solar energy reaching the Earth's surface in one hour exceeds the annual need of all humanity for energy. This fact causes that solar energy is one of the most attractive sources of renewable energy and an inspiration for scientists in searching for and developing ways to detect it, convert it into a useful form of electricity and storage.

Nearly all plants, some simple eukaryotic organisms (such as dinoflagellates, diatoms or brown algae) and some bacteria such as cyanobacteria, green or purple bacteria have the ability to carry out the photosynthesis process. This process in the light-dependent phase begins with the absorption of solar radiation by organic molecules found in thylakoids, the basic elements of a plant cell chloroplast or autotrophic prokaryotic cell, called assimilation dyes. These molecules are located in protein-lipid matrices creating more or less extensive protein photosynthetic complexes. Photosynthetic organisms use pigment-protein complexes to absorb sunlight, to efficient energy transfer and to charge separation across the photosynthetic membrane. Nature has optimized this process so much that the efficiency of one electron separation cycle per absorbed photon of sunlight is close to unity. The charge separation takes place in reaction centres (RC) of photosynthetic complexes: photosystem I (PSI) and photosystem II (PSII) [3]. Due to its unique properties, these complexes have found application as components of systems such as photosensors [4,5], biosensors for detection of herbicides [6], and solar devices [7,8].

Metal nanoparticles are characterized by a strong absorption of light in the visible and ultraviolet range, thanks to which they have been successfully used for thousands of years in the production of stained glass or ceramic vessels. A well-known example of this is the ancient Lycurgus cup, probably from the 4th century AD, which now is placed in the British Museum in London. The vessel changes colour depending on the light exposition, namely in the reflected light it is green and in the light transmitted by it has a red colour (Fig. 1a, b). And although this unusual vessel was created hundreds of years ago, it was only the development of microscopic techniques that allowed scientists in 1990 to use a transmission electron microscope (TEM) to explain this phenomenon. The material from which the cup was made is dichroic glass, containing gold (Au) and silver (Ag) particles with a diameter of about 50-100 nanometers (Fig. 1c) [9].
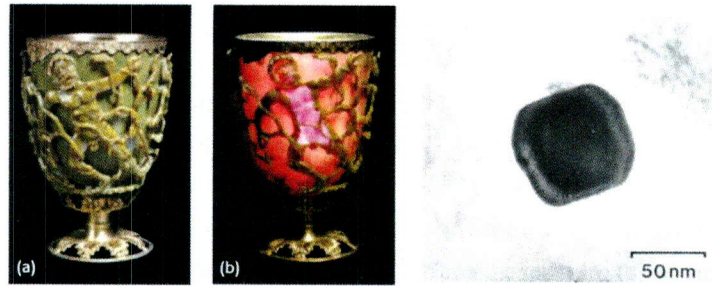
Fig. 1. The Lycurgus cup: in reflected light (a), transmitted light (b) TEM image of the silver and gold alloy nanoparticle (c) [9].

The colour changes of the vessel occur due to the localized surface plasmon resonance (LSPR) found in the metallic nanoparticles. As a result of the interaction of the electromagnetic wave with the free electrons from the conductivity band Ag and Au, the oscillation of free electron gas is induced. The quasiparticle that is the quantum of such oscillations is called plasmon. The position of the plasmon resonance band depends on the material from which the metallic nanoparticle is made (gold, silver, platinum, etc.), its shape and size. For example, Fig. 2 shows TEM images of gold nanorods coated with CTAB polymer, with different ratio of length to diameter (a-d) corresponding to them plasmon resonance absorption bands (e) and dependence of that ratio on the maximum position of the plasmon resonance band (LPM) (f) [10].
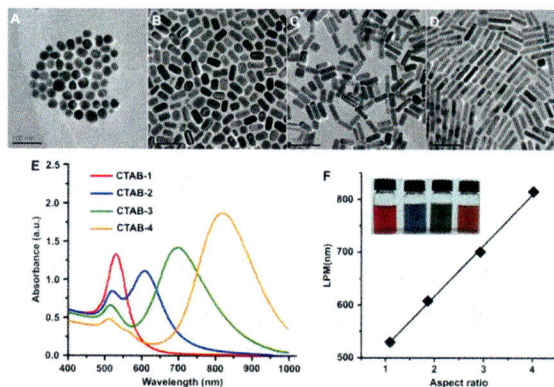
Fig. 2. TEM image of gold nanorods with different aspect ratio of „length x diameter" [nm]: 33x30 (a), 40x21 (b), 50x17 (c) i 55x14 (d) corresponding absorption spectra (e) and dependence of LPM on aspect ratio (f) [10].

The surface plasmon resonance (SPR) phenomenon is used in plasmonic hybrid nanostructures that consist of at least two elements, where one is a metallic nanoparticle and the other any light emitter, e.g. a dye molecule or a photosynthetic complex. One of the main goal of the construction of such hybrid is to obtain a system with improved optical properties. This modification may increase the probability of light absorption by molecules located near the metallic nanoparticles and enhance their fluorescence (MEF – metal enhanced fluorescence). The phenomenon of MEF strongly depends on the wavelengths and distance between the emitter and the metallic nanoparticle [11]. Fig. 3a presents the dependence of enhancement factor (EF) in function of the wavelengths for nanoparticles placed 10 nm from the emitter. The dependence of the fluorescence enhancement coefficient

4

as a function of the mutual distance of the components of the plasmonic hybrid nanostructure, determined on the basis of theoretical calculations, is shown in Fig. 3b.
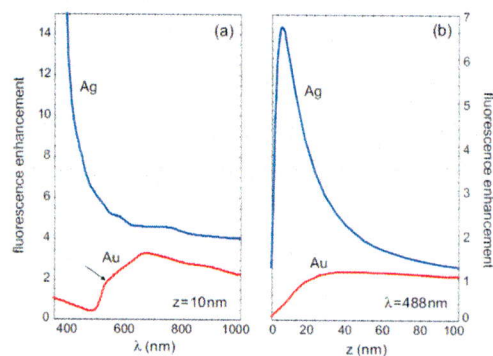
Fig. 3 The calculated fluorescence enhancement factor of a single dye molecule in the vicinity of a silver and gold spherical nanoparticle with a diameter of 80 nm: in the function of: (a) excitation wavelength at a constant mutual distance of 10 nm; (b) the mutual distance at a constant excitation wavelength [11].

Too little distance between the emitter and metallic nanoparticle leads to quenching of the emitter's fluorescence. This happens as a result of the non-radiative transfer of excitation energy to the metallic nanoparticle and then its dissipation. The most efficient MEF is at a distance of about 10-15 nm between the emitter and the metallic nanoparticle, while for larger distance the effect decreases to zero. The MEF is used to increase the quantum yield of fluorescent molecules with the fluorescence quantum yield significantly lower than one.

2. Motivation and objectives

The SPR finds application in medicine [12] or optoelectronic devices [13] allowing to significantly improve the sensitivity and efficiency of the device without increasing its size. The coupling of photosynthetic complexes with metallic nanoparticles can lead to modification of their optical and electrochemical properties. Govorov and Carmeli in 2007 analyzed the effect of the presence of spherical metallic nanoparticles on PSI electron generation efficiency [4]. Theoretical calculations indicate that for the PSI complex combined with the silver nanoparticle, we can expect a strong spectral dependence of the photocurrent generation and a large, fourfold enhancement of photocurrent generation for the excitation energy corresponding to plasmon resonance in the nanoparticle. In addition, Raoul Frese and colleagues presented in 2016 the results of experimental research showing more than double enhancement of photocurrent generated by the bacterial reaction centre (RC-LHI) deposited on nanostructured silver substrate [14]. Such promising results of both, theoretical and experimental work, are inspiration for the study and explanation of the influence of metallic nanoparticles on the optical properties of photosynthetic complexes.

The main goal of my research was to understand the effect of the presence of silver nanoparticles on the optical properties of photosynthetic complexes. For this purpose, one type of metallic nanoparticles - silver nanowires (AgNWs) and photosynthetic complexes with different protein complexity and number of chlorophyll a (Chl a) molecules were selected. First, the interaction of peridinin-chlorophyll-protein (PCP) with silver nanowires was studied. PCP is a simple model protein which monomer contains two Chl a molecules.

In the next step, the bioconjugation process of the PCP complexes with the modified surface pf AgNWs was observed, consisting in the formation of a stable connection streptavidin-biotin. Further research was carried out on functional complexes (capable of transporting electrons) and at the same time with a higher degree of complexity of the photosynthetic protein. Conjugates of the bacterial reaction centre and plant photosystem I were prepared with a modified silver nanowires using the histidine-NTA combination. The obtained hybrid structures were mainly studied by fluorescence microscopy techniques.

The fascination of coupling photosynthetic complexes with metallic plasmonic nanostructures was initiated by Professor Sebastian Mackowski, head of the Optics Team of Nanostructures Hybrids (ZONH) at the Nicolaus Copernicus University in Toruń. I joing to his group in 2011 and it resulted in: knowledge of new experimental methods based on fluorescence microscopy, independent synthesis of silver nanoparticles and nanostructures as well as research on understanding the optical properties of photosynthetic proteins in the presence of metallic nanoparticles.

Research leading to the understanding of optical properties of biohybrid plasmonic nanostructures also required the organization of a new chemical laboratory and the construction of a glove box for carrying out chemical reactions under anaerobic conditions. They were also an inspiration to attempt to extend the functionality of the fluorescent wide field microscope by combining it with a quartz oscillator (tuning fork) enabling precise electrical measurements using the Kelvin Probe Force Microscopy (KPFM) technique.

3. Materials and methods

Studies on the influence of plasmonic interactions on the optical properties of photosynthetic complexes in biohybrid nanostructures were mainly carried out using fluorescence optical microscopy. The basic measurements to determine the concentration or control of photosynthetic protein degradation in aqueous solutions were made by steady-state spectroscopy using a single beam spectrophotometer Cary50 (Varian) and a Fluorolog 3 spectrofluorimeter (Jobin-Yvon).

The hybrid nanostructures, which are my scientific achievement, consist of metallic nanoparticles (silver nanowires) and photosynthetic complexes. Silver nanowires were obtained by chemical synthesis by polyol method [15]. Their average length is about 10 microns, and typical diameters are in the order of tens of nanometers. A scanning electron microscope (SEM) image of nanowires is shown in Fig. 4.
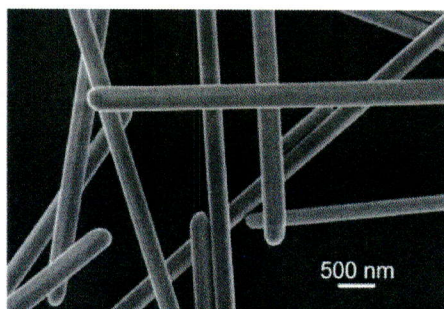
Fig. 4 SEM image of silver nanowires.

6

The maximum of the AgNWs plasmon resonance band is around 380 nm, extends towards the infrared and overlap with the absorption and emission spectra of selected photosynthetic complexes. The micron length of nanowires ensure their simple and precise localization in measurements using an optical fluorescence microscope. The method of deposition of protein complexes on the AgNWs depends on the type of experiment carried out:

a) PCP mixed – solution of PCP with AgNWs in PVA mixed and deposited on the glass substrate,

b) PCP layer by layer (lbl) – the glass substrate was first coated with an AgNWs layer and then covered with a PCP layer in the PVA polymer,

c) PCP@AgNW – PCP bioconjugate with AgNW. PCP complexes with embedded streptavidin were conjugated with a biotin-modified AgNW surface and applied to a glass substrate,

d) RC@AgNW – bioconjugate of bacterial reaction centre (RC) equipped with a histidine tag (Histag) with modified surface of silver nanowires (using nitrilotriacetic acid (NTA) and nickel Ni (II) salt) by forming a coordinate covalent bond between nickel ions and histidine (Ni-His),

e) PSI-LHCI@AgNW – bioconjugate of photosystem I supercomplex with light-harvesting complex I (isolated from red algae) with NTA-Ni modified AgNW surface via cytochrome c_{553},

f) PSI-LHCI+AgNW – PSI-LHCI deposited on NTA-Ni modified AgNWs by the physisorption in absence of cytochrome c_{553}.

One of my important scientific achievements of the presented work was the development of a protocol for silver nanostructures functionalization using NTA-Ni groups. That protocol allows to conjugate His-Tag photosynthetic proteins with AgNWs. Three procedures with a different composition of reagents were chosen after detailed study of the literature. The first one is a two-stage method using 3,3'-Dithiobis[N-(5-amino-5-carboxypentyl)propionamide-N,N'-diacetic acid] dihydrochloride and nickel sulfate [16]. In the second method, the surface of the nanoparticles is first modified with the amino-reactive cross-linking agent DTSP, then exposed to amino-nitrilotriacetic acid (ANTA) which results in attaching NTA moiety to the nanowire surface via a sulfhydryl group at the other end. Finally, the nickel salt is applied [17]. The third method come down to the formation of a NTA-Ni group on the metal surface in five steps [18]. Because the chemical compounds used are reactive with oxygen, in order to achieve better results, a glove box was constructed on its own (Figure 5), in which in the inert gas (argon) environment several steps of surface modification of silver nanoparticles were carried out. The best results of AgNW bioconjugation with RC and PSI photosynthetic proteins were obtained using the second procedure.

Fig. 5 Handmade glovebox from my project at NCU.

In the first step, 250 µL of an AgNW aqueous solution (OD = 8.0 at λ = 380 nm) was centrifuged and rinsed with dimethylsulphoxide (DMSO). The silver nanowires were then placed in a solution of cross-linking agent DTSP (dithiobis succinimidyl propionate) in DMSO at a concentration of 1 mg/mL. After an incubation time of 60 minutes, the AgNWs were centrifuged and rinsed with a 0.5 M aqueous solution of potassium carbonate (pH 9.8) and left for 90 minutes in a mixture of 150 mM chelator (Nα, Nα-Bis (carboxyMethyl) -L-lysine) at 0.5 M K_2CO_3. The described procedure for surface modification of nanowires was carried out in a glove box under argon, and its scheme is shown in Fig. 6. Finally, after centrifuging the solution, AgNWs were placed in ultra-pure distilled water. Incubation of photosynthetic complexes with modified nanowires will be described later in the result chapter.
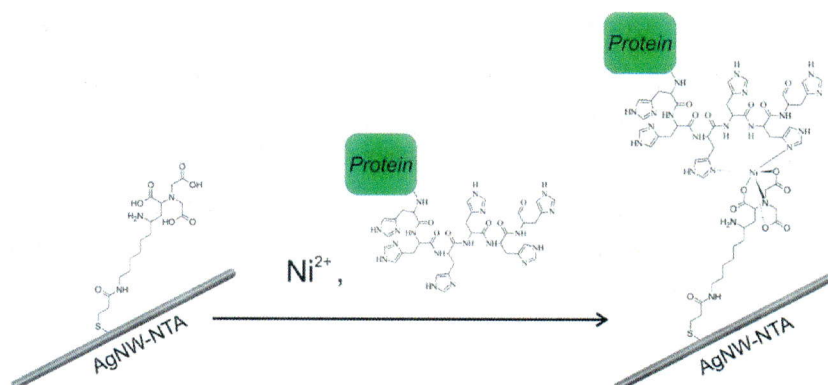
Fig. 6 Scheme of the AgNWs modification procedure using NTA-Ni groups and conjugation with a photosynthetic complex equipped with His-Tag.

Experiments for understanding the influence of metallic nanoparticles on the optical properties of photosynthetic complexes were carried out using two fluorescence optical microscopy techniques: wide field microscopy and confocal microscopy. Both microscopes in ZONH are based on Nikon microscope body and components. A fluorescence wide field microscope was integrated with an atomic force microscope (AFM) based on a quartz resonator with its controller. The mechanical system for integration of microscopes consists of the base of the AFM microscope, moved in two axes (x, y) of the table equipped with travel motorized actuators and sample holder. The mechanical part of AFM microscope consists of a quartz resonator holder, tri-axial (x, y, z) piezoelectric table and feed equipped

8

with a piezoelectric screw together with the controller. Described microscope is presented in Fig. 7.
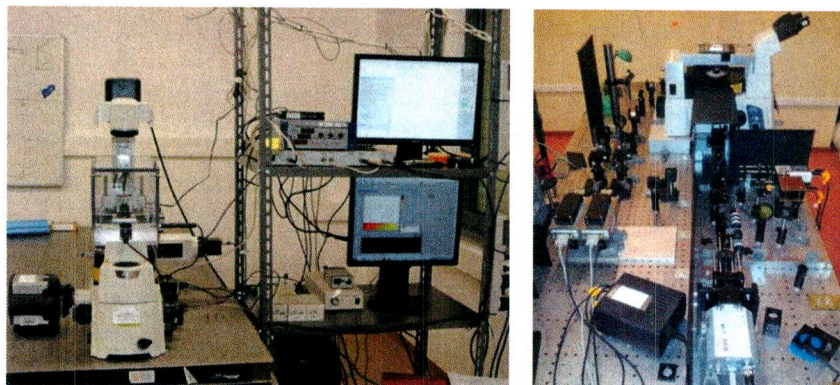
Fig. 7 A photo of a wide field microscope extended with an AFM scanner (left) and a confocal microscope (right).

This wide field microscope made it possible to measure the fluorescence intensity maps of the biohybrid nanostructures and their topography using the AFM method. A confocal fluorescence microscope was used to study both fluorescence intensity maps of hybrid systems with their emission spectra and fluorescence decay curves using the Time Correlated Single Photon Counting (TCSPC) method. The combination of two microscopy techniques, a fluorescent wide field with atomic microscopy, allowed to study the topography of the discussed hybrid nanostructures, precisely locate silver nanowires, estimate their size, etc., and study the enhancement of fluorescence intensity of photosynthetic complexes coupled to nanowires. In addition, the use of confocal fluorescence microscope allowed for additional information on the nature of the interaction of protein complexes with silver nanowires.

4. Experimental results

[H1] *"Imaging of fluorescence enhancement in photosynthetic complexes coupled to silver nanowires",* 2013, Applied Physics Letters, 102, pages: 083703/1-083703/5

The peridinin-chlorophyll-protein (PCP) is a light-harvesting complex isolated from algae *Amphidinium carterae* from dinoflagellate [19]. Figure 8a shows the crystallographic structure of PCP monomer which consists of two protein chains embedded in a protein-lipid matrix (blue).

a)

b)
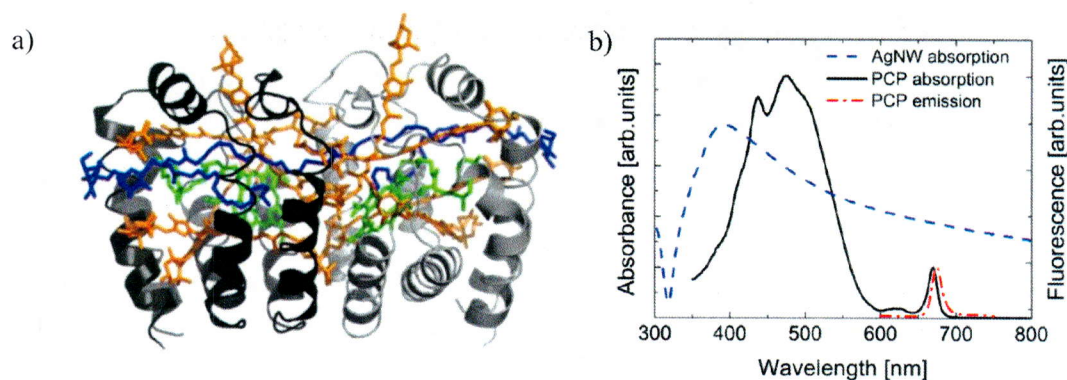
Fig. 8 Crystallographic structure of PCP monomer [20] (a) and absorption spectrum (black line) and fluorescence spectrum (red line) of PCP, excitation wavelength 532 nm [21] (b).

Four molecules of peridinin connected with van der Waals bonds are embedded in each chain (orange colour) and are surrounding one chlorophyll *a* molecule (green colour). The PCP complex is characterized by the absorption spectrum shown in Figure 8b with black colour. Peridinin absorbs light in the range from 400 nm to 550 nm and transfers energy to the Chl *a* molecule, which collects light in the Soret band with a maximum around 440 nm and in the area from 600 nm to 670 nm. The fluorescence spectrum of PCP marked in red in the figure has a maximum at the wavelength of 673 nm which corresponds to the emission of Chl *a*. Due to its simple structure, i.e. relatively low protein complexity and small amount of photosynthetic dyes, PCP is a good model complex. Figure 8b also shows a blue dashed line of extinction of silver nanowires that overlaps with the absorption and emission spectrum of the PCP, with the maximum of the plasmon resonance band located at about 380 nm.

In order to investigate the effect of the presence of silver nanowires on the optical properties of PCP complexes, a mixture of an aqueous protein solution and an aqueous AgNWs solution containing a PVA polymer was prepared. This resulted in an AgNWs water mixture with PCP at a protein concentration of 1 µg/mL in 1% PVA, which was spin coated on a coverslip with speed of 60 rounds per second. The prepared sample was called "mixed", while the reference sample was obtained in an analogous manner by adding distilled water instead of the AgNWs solution to the mixture. The use of PVA polymer was aimed at creating a homogeneous layer of PCP, and it also reduced the effect of PCP's photobleaching (photochemical irreversible process of Chl *a* molecules transition into a non-fluorescent state). Samples were excited by LED illuminators with 405 nm and 480 nm light (in the case of measurements using a wide field microscope) and by laser with 485 nm (in

10

the case of experiments on a confocal microscope). This excitation wavelength corresponding to the maximum of PCP absorption band and at the same time is just behind the maximum of plasmon resonance band of silver nanowires.
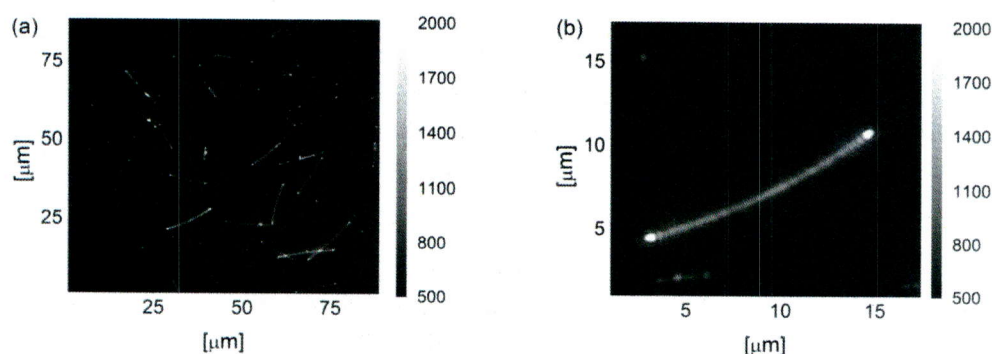
Fig. 9 Wide-field microscopy images of fluorescence obtained for PCP complexes deposited on Ag nanowires. The excitation of 405 nm was used.

The example of fluorescence intensity map of PCP complexes for a "mixed" sample is shown in Fig. 9a. This map is collected exceptionally for the excitation wavelength of 405 nm, which is located closer to the maximum of the AgNWs resonance band. For all the rest of the experiments and data analysis the excitation of 480 nm was used. It can be noticed that emission of PCP complexes is enhanced in the area of AgNWs compared to the PCP emission on glass. Fig. 9b shows the zoom in for one, well separated silver nanowire covered with PCP proteins. Fluorescence intensity of photosynthetic complexes placed away from the nanowires is much lower than for the complexes coupled to AgNWs. Moreover, the this emission intensity is clearly higher at the ends of the silver nanowires. This situation has been observed for over 90% of the analysed PCP coupled to silver nanowires. The strong plasmonic effect observed at the ends of nanowires can be due to antennae effect, where higher density of electromagnetic field is expected for structures with high curvature as well as due to enhanced scattering of plasmons in nanowires at discontinuities. The procedure of analysis data was focused on estimating the fluorescence intensity for the PCP complexes placed along the nanowires and at their ends. In that case the value of emission intensity was taken as an average fluorescence intensity obtained from all pixels along a curve that followed the individual shape of each NW. By placing identical curve to the vicinity of the analysed AgNW (where the fluorescence was not enhanced) the reference intensity was obtained. The ends of nanowires were analysed analogically from single, brightest points. The ratio of PCP emission obtained in this way is the plasmonic enhancement factor (EF) of PCP emissions in the presence of silver nanowires. The value of averaged enhancement factor is 1.1 and 2.2 for PCP complexes located along the nanowires and at the ends of AgNWs, respectively.

Measurements of PCP emission intensity maps for a "mixed" sample obtained with wide field fluorescence microscopy technique showed enhanced emission of photosynthetic complexes located in close vicinity to metallic nanoparticles. Unfortunately, this technique does not allow to explain, whether this enhancement is only result of enhanced light absorption in the hybrid system. More direct information about the nature of plasmonic interactions in presented hybrid nanostructures can be derived by measuring the

fluorescence spectra and emission decay curves. Consecutive measurements were made using the fluorescence confocal microscopy technique. Then, in confocal mode, PCP complexes were localized precisely along the selected nanowires, at their ends or in non-interacting with AgNWs neighbourhood, and for this particular setting the emission spectrum and PCP fluorescence decay curves were recorded.
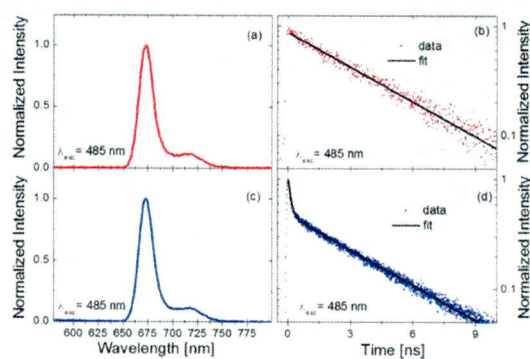
Fig. 10 Emission spectra (left) and the corresponding fluorescence decay curve (right) for PCP complexes placed outside of AgNWs (a and b) and on AgNWs (c and d) at excitation 485 nm. Experimentally measured transient curves were fitted with exponential decays, as displayed with solid black lines.

In Fig. 10, the results for the reference sample and for the photosynthetic complexes located in close vicinity to the silver nanowires are shown in red and blue respectively. The PCP emission spectra do not change their shape, which means that the protein in contact with the metallic nanoparticle remains intact - its structure is not changed and it is not damaged. A clear difference is visible for the PCP fluorescence decay curves. In the absence of a metallic nanoparticle, the decay of PCP complexes is mono-exponential with a typical decay constant of about 4 ns, remaining in agreement with previous studies [22]. For the PCP complexes coupled to nanowires, a bi-exponential fluorescence decay is observed. One component of this decay is characteristic for PCP lifetime in the absence of a metallic nanoparticle, while the second component has a value of less than 0.3 ns. More than a ten-fold reduction of the radiative rate of Chl a molecules in the PCP complex is due to the interaction with plasmons induced in silver nanowires.

In conclusion, in this work a model PCP photosynthetic complexes were successfully coupled to silver nanowires and an almost two-fold enhancement of protein emission was observed. Interactions between PCP complexes and AgNWs resulted in an increased value of fluorescence intensity and shortened lifetime of photosynthetic complexes. These were the first such results on a global scale.

Studies on PCP complexes coupled with silver nanowires were continued for two concentrations of PCP complexes differing in order of magnitude ($c_1 = 2$ µg/mL and $c_2 = 0.1$ µg/mL), two excitation wavelengths (405 nm and 480 nm) and two geometries of samples - "mixed" and "layer by layer" (lbl). Excitation wavelengths of hybrid nanostructures have been selected to excite PCP complexes around their maximum of absorption band (480 nm) and in the vicinity of the maximum plasmon resonance band of silver nanowires (405 nm). To observe the most efficient MEF of PCP complexes two different concentrations of photosynthetic proteins were selected (while maintaining the same AgNWs concentration). Because the phenomenon of MEF strongly depends on the distance between the metallic nanoparticle and the emitter, the experiment used two types of sample geometry presented in Fig. 11. In the case of a "lbl" sample, a layer of nanowires deposited on the glass substrate was covered by a PCP layer (Fig. 11 a) whereas the "mixed" sample was a mixture of both these components, applied to the glass substrate (Fig. 11 b).
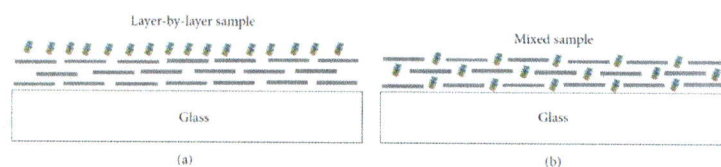
Fig. 11 Geometry of the "lbl" sample (a - left) and "mixed" sample (b - right) on the glass substrate. Gray dashed lines represent AgNWs, and coloured objects are PCP complexes.

Collected emission intensity maps of PCP complexes for the discussed hybrid structures showed an increase in the fluorescence intensity of the protein in the close vicinity of AgNWs. Analysis of PCP fluorescence intensity maps was performed analogously to the previous publication. Fig. 12 shows the histograms of the fluorescence enhancement factor of PCP complexes coupled with AgNWs and excited at 405 nm. The blue sample was marked "mixed" and the red sample "lbl". Due to the fact that at the ends of nanowires, the photosynthetic complexes exhibit a much higher emission intensity, the determined EF values were placed on separate histograms (Fig. 12 b and d). The upper panel of the figure refers to a concentration of 2 µg/mL of protein and the lower panel presents results for the lower concentration. The average values of PCP emission enhancement factor for a "mixed" ("lbl") samples with a higher protein concentration are 1.32 (1.22) for complexes located along nanowires and 2.40 (1.67) at their ends, respectively. The influence of sample geometry on EF values is more dominant for samples with lower concentrations. In this case, the average values of EF for the "mixed" ("layered") samples are 1.93 (1.22) along AgNWs and 4.11 (1.73) at their ends, respectively.
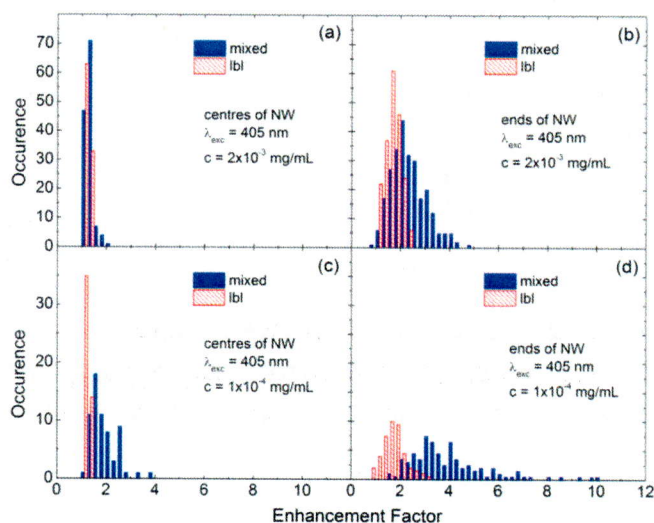
Fig. 12 Histograms of EFs for the „mixed" (blue) and „layer by layer" (red) samples. On the right, the analysis was carried out for complexes deposited at the ends of AgNWs, on the left for proteins located along the AgNWs. PCP concentration: 2 μg/mL (a and b) and 0.1 μg/mL (c and d); λ_{exc} = 405 nm.

An analogous analysis was carried out for samples excited by light at 480 nm. In this case, the calculated averaged values of EF for the "mixed" ("layered") samples, with a higher protein concentration, along AgNWs were 1.35 (1.25) and at their ends 2.32 (1.76), while for the sample at a lower concentration, they were 2.10 (1.27) along metallic nanoparticles and 4.83 (2.04) at their ends, respectively. The obtained results using the wide-field microscope are only qualitative and approximate, and obtained EFs of PCP emission are usually underestimated. In order to estimate the more quantitative nature of PCP interactions with AgNWs, emission spectra of photosynthetic complexes isolated from metallic nanoparticles and coupled with silver nanowires as well as their decay curves were measured. The emission spectra of PCPs coupled to AgNWs, regardless of the geometry of the sample, have the same shape and position as the fluorescence spectra of proteins in the absence of metallic nanoparticles. This means that the photosynthetic complexes coupled to AgNW retains its functionality and is not damaged.
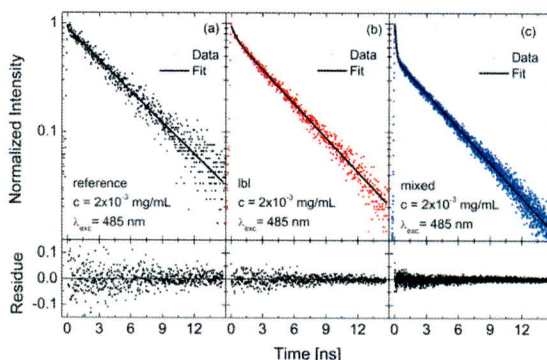
Fig. 13 The PCP fluorescence decay curves together with fits of exponential functions and residuals for reference (a), "lbl" (b) and "mixed" (c) samples. PCP concentration:: 2 μg/mL, λ_{exc} = 485 nm.

Figure 13 shows PCP emission decay curves. In the case of the reference sample, the exponential decay of emission with the determined fluorescence lifetime value is visible, 4

14

ns irrespective of used excitation wavelength - 405 nm and 485 nm. For both hybrid nanostructures is observed a bi-exponential fluorescence decay of PCP complexes. Obtained the fluorescence lifetimes of protein complexes coupled to silver nanowires are about 4 ns and 0.3 ns for the "mixed" sample regardless of used excitation wavelength. In the case of a "lbl" sample, the shorter lifetime was 0.2 ns for excitation 405 nm and 0.5 ns for excitation 485 nm. In addition, in the case of a "mixed" sample, the amplitude associated with the fitting of the two-exponential function for a smaller value of the decay time constant is two times higher as in the case of the "lbl" sample. It means that the number of PCP complexes interacting with nanowires is larger for the "mixed" sample. The long component measured for the laser beam placed onto a nanowire originates from the PCP complexes that are isolated from the nanowire. The diameter of the laser spot is about 1 μm and the diameters of the AgNWs below 200 nm. Due to that fact it is expected to detect signal associated with the PCP complexes that are far away from nanowire and do not interact with it.

In summary, the presented study observed a plasmonically enhanced fluorescence of PCP complexes conjugated to silver nanowires. The EFs values do not depend on used excitation wavelengths. The geometry of the sample and the concentration of photosynthetic complexes affect the observed increase in the emission intensity of PCP complexes. In the case of a "mixed" sample, a larger number of protein complexes interact with metallic nanoparticles. The shortening of PCP fluorescence lifetime indicates that the increase in the radiative constant plays an important role in the presented hybrid nanostructures. The obtained results can be applied for developing ways to plasmonically control the light-harvesting capability of photosynthetic complexes.

[H3] *"Wide-field fluorescence microscopy of real-time bioconjugation sensing"*, 2018, Sensors 18, 290, pages: 1-10

As mentioned before, the plasmonic interactions between the emitter and the metallic nanoparticle depends on the distance between them and the phenomenon of enhanced fluorescence requires their mutual distance between 10 nm - 30 nm. Due to that fact, another research challenge was set up to control the distance between PCP complexes and silver nanowires. The protocol for the modification of the surface of silver nanowires using biotin was used from the doctoral dissertation M. Olejnik [23]. PCP complexes with attached streptavidin protein (PCP-strept) were conjugated with AgNWs by forming a streptavidin-biotin binding. Using wide-field microscope, the speed rate of the bioconjugation process was studied. Fig. 14 (a) shows a photo of white light transmission for a sample with silver nanowires deposited on clean bare glass. After 10 seconds from the start of collecting data, 5 μL of PCP-strept solution with a concentration of 0.2 μg/mL was applied and changes in the fluorescence intensity of the protein complexes were observed.
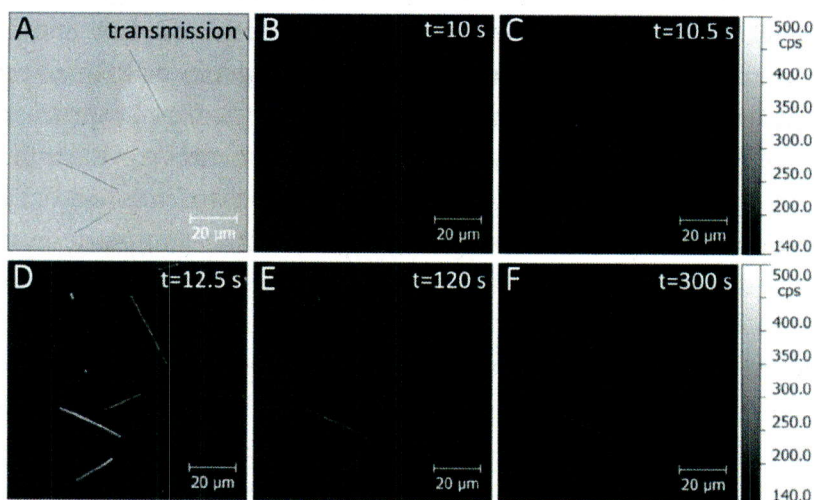
Fig. 14 Transmission image of AgNWs before application of PCP solution (a), PCP fluorescence intensity map straight after application of PCP solution (b) and PCP emission intensity maps recorded in the described time of measurement collection. The scale of PCP emission intensity on all maps is identical; λ_{exc} = 405 nm.

The measurements show that the intensity of light from the emission of PCP complexes deposited on the modified surface of nanowires begins to appear after 0.5 s from application of protein solution. This intensity reaches its maximum value after 2.5 seconds from the application and then starts to decrease as a result of the slow photobleaching process. In order to investigate the influence of the substrate (on which the sample was placed) on the dynamics of the conjugation process, the glass substrates modified with streptavidin were used and the experiment was repeated. Biotin-modified silver nanowires were applied to a streptavidin glass and the PCP-strept solution was applied.
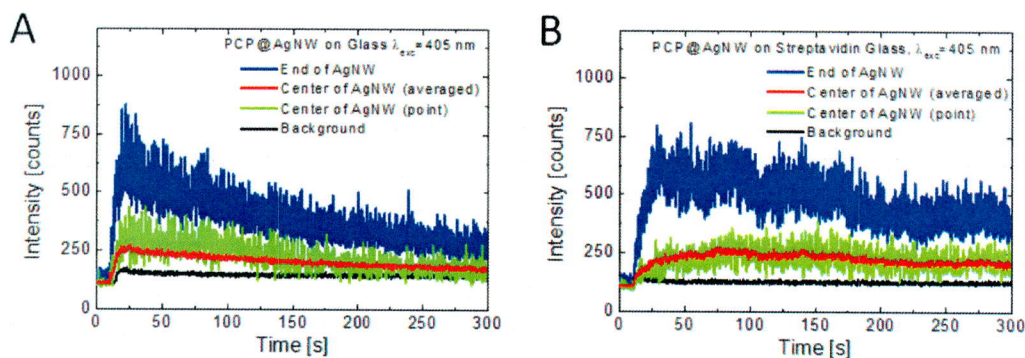
Fig. 15 Kinetics of PCP@AgNW emission intensity changes: on glass (a) and streptavidin glass (b). Changes in the emission intensity of PCP complexes conjugated at the ends of AgNW (blue), along the AgNW (red - average value from the entire length of the nanowire, green - value from one point on the nanowire), outside the AgNWs area (black).

Fig. 15 shows the kinetics of changes in the fluorescence intensity of PCP complexes conjugated with nanowires deposited on clean glass and on streptavidin glass. The changes in the intensity of protein emission located at the ends of nanowires are blue, while the emitters deposited on the glass outside the area of interaction with the silver nanoparticles are marked with black. For PCP located along the nanowires, red was used for the average emission intensity collected from the entire AgNW length, and the green value of the

fluorescence intensity collected from one point on the nanowire was used. In both cases of used substrate, an increase in the PCP emission intensity conjugated with AgNW was observed, followed by its decrease as a result of the photobleaching process of chlorophylls. Moreover, in the case of streptavidin glass substrate no signal is obtained from the emission of free PCP complexes (reference from outside the interaction area with AgNW)). This can be explained by the repulsive action of the glass substrate on which streptavidin protein molecules are deposited relative to the PCP complexes, which also contain streptavidin attached. It is possible that PCP complexes remain for a longer time in the applied solution "waiting for" attachment to the modified AgNW surface, which could explain the longer rise time of PCP emission intensity located on AgNW, deposited on the streptavidin substrate compared to the situation on the glass substrate. In addition, a detailed analysis of approximately 60 well-separated nanowires on both substrates showed that the average PCP emission along AgNWs (at the ends of AgNW) on a clean glass substrate is 540 ± 190 (1700 $\pm$ 600) while on a substrate modified with streptavidin is 230 ± 60 (700 ± 300).

In summary, the described work uses a wide field fluorescence microscopy technique to monitor the bioconjugation process of silver nanoparticles with photosynthetic complexes. The bioconjugation process is very efficient and takes place in just a few seconds. The speed of the bioconjugation process on the substrate modified with streptavidin is smaller compared to pure glass. On both substrates there is a phenomenon of plasmonically enhanced emission of PCP complexes conjugated with AgNWs. This method could be universally applied for real-time biochemical sensing with metallic, plasmonically-active nanostructures or platforms, presumably down to single protein level.

[H4] ***"Spectrally selective fluorescence imaging of Chlorobaculum tepidum reaction centers conjugated to chelator modified silver nanowires"***, 2018, Photosynthesis Research, 135, pages: 329-336.

The research presented earlier has allowed to describe the effect of the presence of metallic nanoparticles on the optical properties of a simple protein complexes. The Reaction Center (RC) is a natural light converter found in the cells of photosynthetic organisms. It shows almost 100 % of quantum efficiency of light conversion to electric current. This fact causes that many scientists around the world make attempts to incorporate this type of protein complexes into various types of electrodes to construct cheap and effective photovoltaic cells. The coupling of such protein complexes to silver nanoparticles can lead to modification of their optical properties. This in turn may translate into increased efficiency of absorbed solar radiation or efficiency of photocurrent generation by bioelectrodes constructed on the basis of functional photosynthetic complexes. In addition, as a result of such a combination, a structure with an oriented location of photosynthetic complexes should be created, working as an anode or cathode, depending on the orientation of the functional photosynthetic complexes to its surface.

In this work, a reaction centers from green bacteria *Chlorobaculum (Cb.) Tepidum* is used, which is a transmembrane pigment-protein super complex and, at the same time, a simpler analogue of photosystem I (PSI). Fig. 16 shows the absorption spectrum of RCs (green) and AgNWs (black) and the emission spectrum of reaction centers (red).
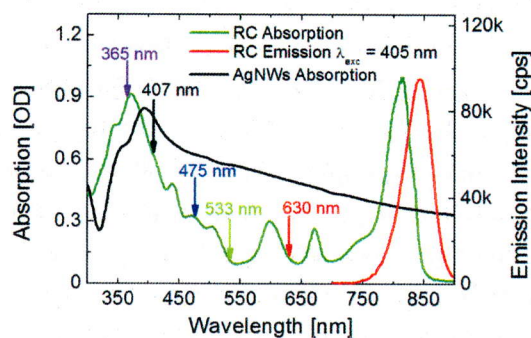
Fig. 16 Absorption spectra of RCs (green) and AgNWs (black) and emission spectrum of RCs (red). Arrows indicate excitation wavelengths used in the experiment.

Carotenoids absorb light in the range between 430 nm and 540 nm. Contribution of bacteriochlorophyll *a* (BChl a) in the absorption spectrum of RCs is visible in two spectral regions from 300 nm to 430 nm and between 540 nm and 850 nm (the Q_x and Q_y bands are visible at around 600 nm and 810 nm). The absorption band, whose maximum is about 670 nm belongs to the Chl *a* derivative. The FMO (Fenna-Matthews-Olson) protein is attached to the RC complex, which BChl *a* absorbs light in the spectral range from 550 nm to 645 nm. Light absorbed by the FMO protein is mainly transferred to the RCs. The emission spectrum of RC is characterized by a wide band with a maximum located at around 840 nm. Widening of this spectrum on the short-wave slope may be the result of FMO fluorescence. The figure also shows the absorption spectrum of silver nanowires, which overlaps with the absorption and emission spectrum of RCs. The RC's complexes are equipped with a polyhistidine bridge (His-Tag), which allows them to be attached in a specific way to the modified surface of nanowires. The process of surface modification of AgNWs with NTA acid and nickel salt has been described in the section on measurement methodology. The modified AgNW-NTA were incubated in a buffer solution with RCs for 60 minutes and then rinsed and centrifuged several times. This procedure ensured that finally only the RC complexes conjugated with the AgNW surface (RC@AgNW) were in the solution.

Fig. 17 presents maps of emission intensity of RC complexes immobilized on the surface of silver nanowires recorded using (a) confocal microscope and (b) wide field microscope. The measured emission spectra of RC complexes attached to AgNWs at various positions on the nanowire are characterized by a different fluorescence intensity value, but their shape and position is the same as for RC complexes in the buffer solution (Fig. 17a). This means that in the bioconjugation process and in the vicinity of metallic nanoparticles, RCs are not damaged or denatured and retain their functionality.
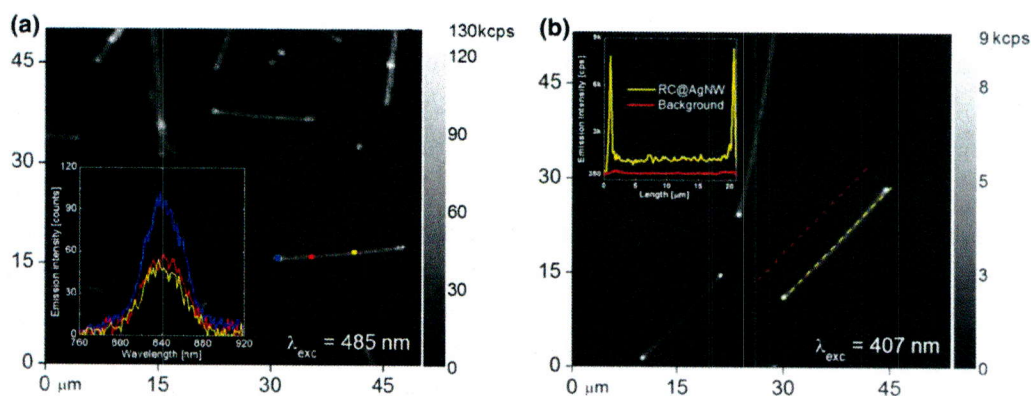
Fig. 17 Fluorescence intensity maps of RC complexes attached to AgNWs collected using (a) confocal microscope (inset: emission spectra of RCs located on particular spot on AgNW) and (b) wide field microscopy (inset: distribution of emission intensity of RCs immobilized along the selected nanowire (yellow color) and its vicinity (red color)).

Fig. 17b displays how the RC's complexes homogeneously immobilized on the AgNW's surface - a bright emission intensity of RCs feature the shape of the nanowire, along with lighter endings on an essentially dark background. Inset shows the distribution of emission intensity of RCs attached along the nanowire (yellow) and practically its lack in the AgNW environment (red color), which means that in the final solution all RC complexes were conjugated with the surface of AgNWs. In addition, the distance between the nanowire and the protein complexes was enough large that there was no quenching of fluorescence of RCs. In order to accurate investigate the effect of the presence of metallic nanoparticles on the optical properties of RC complexes, five excitation wavelengths have been used from the entire absorption of RCs (corresponding to absorption of different protein pigments). The measurements were carried out in such a way that exactly the same spot on the sample was illuminated with a wavelength from 630 nm to 365 nm (using the same excitation power), and emission intensity maps of RC@AgNW were collected. This procedure allowed to determine the relative values of the emission intensity of RCs conjugated to a particular nanowire in the function of excitation wavelength. Over one hundred isolated, well-separated nanowires were analysed.
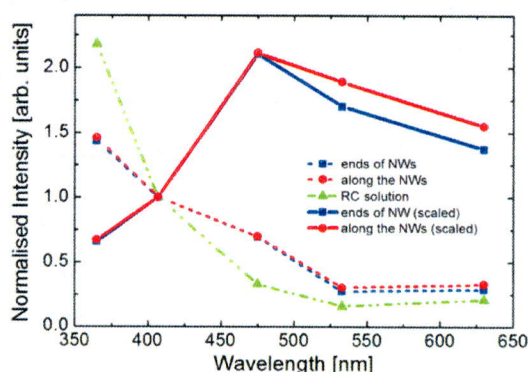
Fig. 18 Comparison of the fluorescence intensity of RC buffer solution (green triangles) and averaged emission intensity of RC@AgNWs at the ends of NWs (blue squares) as well as along the NWs (red circles). Solid lines correspond to emission intensity of RC@AgNWs scaled to the excitation spectrum of RC solution.

Fig. 18 shows the emission intensity of the RC solution in the buffer (green colour) determined from the excitation emission spectrum measured at a constant value of the excitation light intensity. The emission intensity of RC@AgNW conjugates were measured using a wide field microscopy for the same excitation powers of all five LED illuminators used. The average values of emission of RC@AgNWs determined along the nanowires (red dots) and at their ends (blue squares) are marked with a dashed line. All graphs were normalized to the emission of RC at 407 nm excitation. It can be noticed that the dependence of the intensity of light emitted by the RC complexes on the excitation wavelength is different for the case of buffer solution and RCs conjugate with NWs. While the emission intensity of the RC solution has a higher value for λ_{exc} = 365 nm compared to RC@AgNWs, this situation is reversed for λ_{exc} = 485 nm. For a better presentation of the influence of nanowires on the optical properties of RCs, the emission intensity of RC@ AgNWs was normalized to the same value of absorbed light intensity, i.e. divided by the emission intensity values from the RC excitation spectrum in the buffer solution. In this way red and blue solid lines were obtained. One can clearly see the influence of plasmonic excitations induced in silver nanowires on enhancing the emission intensity of RC complexes attached to AgNWs in an oriented way. Additional measurements for RC@AgNW conjugates made with time resolved spectroscopy methods showed that the fluorescence decay curves measured at excitation wavelengths of 485 nm and 640 nm do not differ from emission decay curves for the reference sample (RC solution in buffer). Since there is no shortening of the fluorescence lifetime of the protein complexes immobilized on nanowires, it can be concluded that the increase of emission intensity of RCs conjugated to AgNWs is mainly the result of enhanced absorption of light by RC.

In summary, in this paper Reaction Centers were immobilized on the silver nanowires in an oriented way. Bioconjugation did not quench the emission of RCs, it even enhanced it. Plasmon enhancement of emission of RCs is mainly the result of enhanced absorption of photosynthetic complexes. Obtained results can be applied for the construction of improved solar energy converters based on photosynthetic complexes and metallic nanoparticles. The research described below was conducted as part of the European BoldCats project ("Bioinspired Oxygen evolving Light Driven CATALYSIS (BOLDCATS)", 2011-2014, 650,000 PLN), which I was the main contractor and coordinator of cooperation with the laboratory of prof. R. Cogdell.

[H5] *"Plasmon-induced absorption of blind chlorophylls in photosynthetic proteins assembled on silver nanowires"*, 2017, Nanoscale, 9, pages: 10475-10486

Photosystem I with the light-harvesting antenna complex I (PSI-LHCI) is a super complex protein isolated from red alga *Cyanidioschyzon merolae*. It is characterized by high resistance to extreme conditions such as exposure to light, temperature (20° C - 60° C) or pH (4 - 11), making it an interesting photosynthetic protein for use in, for example, converters of sunlight for electricity [24]. Previous research has shown that the oriented attachment of reaction centers RC to silver nanowires results in a modification of their optical properties. Therefore, in this work, a PSI-LHCI super complex was conjugated with silver nanowires via His-tagged cytochrome c_{553}, which is a natural electron donor. The crystal structure of

PSI-LHCI is well known and is presented in Figure 1a. This super complex form a monomer with a size of 15 nm and contains about 157 - 159 molecules Chl a and 35 molecules of carotenoids. Fig. 1b shows the absorption (black colour) and emission (red colour) spectrum of PSI-LHCI together with the absorption spectrum of silver nanowires (blue colour).

a)   b)
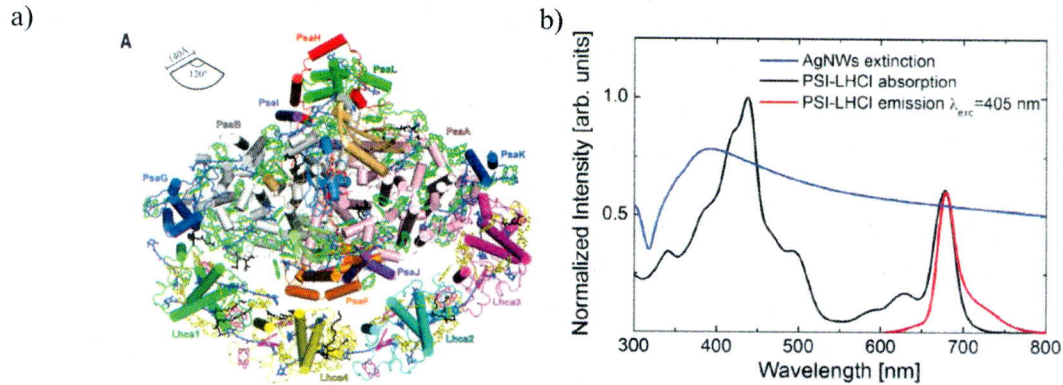
Fig. 19 Crystal structure of PSI-LHCI monomer [25] (a); absorption spectrum (black line) and fluorescence spectrum (red line) of PSI-LHCI for excitation wavelength 405 nm and absorption spectrum of AgNW (blue line) (b).

The absorption spectrum of the supercomplex is characterized by several broad bands that correspond to the absorption of light by various photosynthetic pigments. Chl a molecules absorb sunlight in the Soret band corresponding to the part of ultraviolet and blue light, and near infrared (Q_y band). The absorption of carotenoids is characterized by smaller bands in the region of green light. The maximum of emission spectrum of PSI-LHCI is at 678 nm, and the spectrum is widening towards longer wavelengths which is attributed to the emission of so-called red chlorophylls. The isolated native PSI-LHCI complexes do not have a histidine tag enabling them to be attached in an oriented way to the modified surface of the silver nanoparticles. In this situation, the natural electron mediator - cytochrome c_{553} equipped with His-Tag was used.

a) b) c)
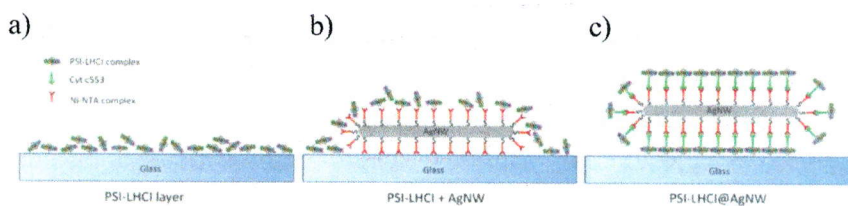
Fig. 20 Geometry of samples: (a) PSI-LHCI layer, (b) PSI-LHCI complexes deposited on AgNW without using cytochrome, (c) PSI-LHCI immobilized on AgNW using cytochrome.

Fig. 20 shows the geometry of investigated samples. The main difference between the samples is the presence of cytochrome c_{553} (PSI-LHCI@AgNW) or its absence (PSI-LHCI + AgNW). In the case of a sample where cytochrome was not used, the protein complexes could not attach to the surface of the silver nanowires in an oriented way, but were only deposited on them by physical adsorption. The modified silver nanowires were first incubated in the cytochrome c_{553} buffer solution for half an hour and then rinsed and centrifuged. The nanowires obtained in this way had the entire surface covered with cytochromes (AgNW-cyt) awaiting for binding of the PSI-LHCI super complexes. First, the

condition required for complete bioconjugation was established. The PSI-LHCl solution was added to the sample containing AgNW-cyt, and after 10 min, 30 min and 60 min of incubation time a mixture was drawn, deposited on glass substrate and emission intensity maps of PSI-LHCl were collected (for 405 nm excitation). The obtained results showed that after ten minutes the PSI-LHCl complexes coupled with AgNW-cyt emit enhanced fluorescence, however, the intensity of this emission is weak and heterogeneous along the NWs. A much better effect was visible after 30 minutes, and after 60 minutes where the emission of PSI-LHCl complexes conjugated with AgNW-cyt was much more intense and homogeneous. This time was considered as the optimal incubation time of the PSI-LHCl mixture with AgNW-cyt and was used for further studies. Two PSI-LHCl mixtures were then prepared, one containing modified silver nanowires and one containing cytochrome coated nanowires. Both mixtures were incubated for 60 minutes, centrifuged several times and rinsed and then deposited on glass substrate. The emission intensity maps of PSI-LHCl collected for these samples are presented in Fig. 21.
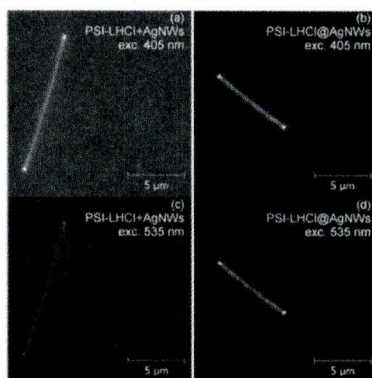
Fig. 21 Emission intensity maps of: PSI-LHCl+AgNW (a, c) and PSI-LHCl@AgNW (b, d) for excitation wavelengths of 405 nm (a, b) and 535 nm (c, d). All maps are on the same emission intensity scale.

The samples were excited using two wavelengths: 405 nm - corresponds to the location of the maximum resonance band of AgNWs and 535 nm - an area in which the PSI-LHCl complexes hardly absorb light. It can be noticed that the presence of metallic nanoparticles in both samples does not quench the emission of super complex proteins. The main difference is in the intensity of emission of PSI-LHCl. The ratio of emission intensity of PSI-LHCl at excitation wavelength 405 nm to emission intensity at 535 nm excitation is: about 5 (PSI-LHCl+AgNW) for samples where photosynthetic proteins were not specifically conjugated with plasmonically active AgNWs in a controlled manner, almost 2 (PSI -LHCl@AgNW) for the conjugates and over 6 for the reference sample (PSI-LHCl). This important result shows that the attachment of PSI-LHCl complexes in an oriented manner to silver nanowires strongly modifies the optical properties of these super complexes. The results of time-resolved fluorescence spectroscopy for these hybrid nanostructures have shown a shortening of the fluorescence decay. Moreover, the bioconjugated nanostructures seems to exhibit the fast component of the fluorescence decay with the slow component significantly diminished. The obtained results show that PSI-LHCl super complexes attached to silver nanowires in an oriented manner have enhanced efficiency of green light harvesting, in the spectral range that those proteins *in vivo* are optically nearly inactive. The reason for this is the strong modification of the optical

properties of these photosynthetic complexes. It should be noticed that illumination of PSI-LHCI above 500 nm populates the so-called red Chlls, which form an energy trap mainly in the LHCI antenna system, but also in the PSI core. The attachment of PSI-LHCI complexes to silver nanowires with their donor side increases the probability of light absorption by red chlorophylls.

In conclusion, in this paper, photosystems I super complexes were immobilized in a oriented way to the modified surface of silver nanowires via cytochrome c_{553}. The time at which the cytochrome c_{553} is connected with the PSI-LHCI complexes was determined. The coupling of PSI-LHCI complexes on the donor side (P700) with silver nanowires modifies the optical properties of these complexes. This modification consists in a strong enhancement of green light absorption, in an area where in natural conditions the light is not nearly absorbed by PSI-LHCI. In this way, we applied oriented nanostructuring of PSI-LHCI complexes to enhance the specific plasmonic interactions that improved absorption of PSI-LHCI, thereby paving the way towards significant advances in the application of this remarkably efficient solar light converter in a viable artificial leaf.

5. Conclusions

The most important results included in my scientific achievement are:

• observation of plasmonically enhanced fluorescence of the simple model photosynthetic complex PCP, coupled as a result of physical adsorption with silver nanowires,

• increasing the effect of the MEF phenomenon for PCP complexes coupled to silver nanowires by controlling the geometry of the sample (increasing the number of protein complexes interacting with nanowires),

• application of wide-field fluorescence microscopy to measure real-time attachment of photosynthetic proteins to plasmonically active silver nanowires,

• enhancement of light absorption by bacterial reaction centers (capable of charge separation) immobilized in an oriented way to silver nanowires,

• development of a protocol for surface modification of silver nanowires and conjugation with them PSI-LHCI super complexes via cytochromes and enhancement of green light absorption by the fabricated hybrid nanostructure.

The presented research results met with great interest of the scientific community in the country and abroad. They were presented in the form of oral presentations and posters at several foreign and national scientific conferences, where they were welcomed. The potential application of the results obtained is:

• for developing ways to plasmonically control the light-harvesting capability of photosynthetic complexes,

• for real-time biochemical sensing with metallic, plasmonically-active nanostructures or platforms, presumably down to single protein level,

23

• for the construction of new, efficient and ecologically clean photovoltaic cells based on functional photosynthetic complexes, capable of charge separation, immobilized in a directed way on the plasmonically active metal nanostructures.

V.   Other scientific/artistic achievements

Immediately after completing my doctoral thesis I went on a post-doctoral internship at the University of Saskatchewan in Canada, where I worked under the supervision of Professor Ronald Steer. The scope of my scientific activity there was a continuation of the subject of my doctoral dissertation. The first experiments carried out in Canada concerned quenching the fluorescence of magnesium and zinc tetraphenylporphyrins by molecular oxygen [26] as well as photophysical properties of these porphyrins in solutions [27]. The next topic was about corroles - porphyrin derivatives. A sudden increase in interest in these compounds appeared when a simple method of their synthesis was discovered. Under the supervision of prof. R. Steer I studied the spectral and photophysical properties of two metallocorroles in a mixture of benzene and pyridine in the ground state and higher excited states [28]. After completing the postdoctoral fellow at UofS in Canada I went to Spain, where at Universidad de La Laguna in Tenerife I cooperated scientifically with the group of Professor I. Martin. I was involved in fabricating glasses and ceramic glasses doped with rare earth ions and studying their optical properties using time-resolved laser spectroscopy [29,30]. After returning to the country, Professor S. Maćkowski offered me a job in his research group, in which I stay up to date. Cooperation with Professor S. Maćkowski turned out to be extremely interesting and interdisciplinary, and the research topic dealt with here focuses on hybrid bionanostructures. In addition to studies on the influence of silver nanowires on optical properties of photosynthetic complexes, I also participated in experiments using other nanoparticles and plasmonic nanostructures in hybrid systems. One of the first works concerned the coupling of quantum dots with PCP complexes [31]. The influence of plasmons induced in the silver island layer (SIF) on the optical properties of photosynthetic complexes with various degrees of protein complexity and number of emitters, such as FMO [32], bacterial reaction center [33] or cyanobacterial photosystem I [34] was also studied. The silver nanowires which I have synthesized have been used successfully in numerous experiments conducted by master students, PhD students and other scientific staff of the ZONH [35]. The interdisciplinary character of ZONH's work was also the result of a precise determination of the quantum efficiency of emissions of thioxinones synthesized in the laboratory of prof. D. Gryko [36] or steady-state spectroscopy of optical properties of organic compounds doped with rhenium and used in organic light emitting devices [37]. I also participated in several grants headed by Professor S. Maćkowski. We are currently working on the already-ending Polish-Turkish project on the study of optical and electrochemical properties of nanostructured bioelectrodes composed of a PSI-LHCI multilayer attached in an oriented manner to the surface of graphene [38] and the influence of the silver islands films deposited under single layer graphene on the electrochemical efficiency of this bioelectrode.

Literature:

(1)   Statistics | World - Total Primary Energy Supply (TPES) by source (chart)
        https://www.iea.org/statistics (accessed Jan 24, 2019).

(2)   Blankenship, R. E.; Tiede, D. M.; Barber, J.; Brudvig, G. W.; Fleming, G.; Ghirardi, M.; Gunner,
        M. R.; Junge, W.; Kramer, D. M.; Melis, A.; et al. Comparing Photosynthetic and Photovoltaic
        Efficiencies and Recognizing the Potential for Improvement. *Science* **2011**, *332* (6031), 805–
        809. https://doi.org/10.1126/science.1200165.

(3)   *Handbook of Photosynthesis, Second Edition*, 2nd ed.; Pessarakli, M., Ed.; CRC Press, 2005.

(4)   Govorov, A. O.; Carmeli, I. Hybrid Structures Composed of Photosynthetic System and Metal
        Nanoparticles: Plasmon Enhancement Effect. *Nano Lett.* **2007**, *7* (3), 620–625.
        https://doi.org/10.1021/nl062528t.

(5)   Terasaki, N. PS-I and PS-II on Electrodes for Energy Generation and Photo-Sensor. *Lecture
        Notes in Energy* **2016**, *32*, 419–449. https://doi.org/10.1007/978-3-319-25400-5_25.

(6)   Swainsbury, D. J. K.; Friebe, V. M.; Frese, R. N.; Jones, M. R. Evaluation of a Biohybrid
        Photoelectrochemical Cell Employing the Purple Bacterial Reaction Centre as a Biosensor for
        Herbicides. *Biosensors and Bioelectronics* **2014**, *58*, 172–178.
        https://doi.org/10.1016/j.bios.2014.02.050.

(7)   Ocakoglu, K.; Krupnik, T.; Van, D. B.; Harputlu, E.; Gullo, M. P.; Olmos, J. D. J.; Yildirimcan, S.;
        Gupta, R. K.; Yakuphanoglu, F.; Barbieri, A.; et al. Photosystem I-Based Biophotovoltaics on
        Nanostructured Hematite. *Advanced Functional Materials* **2014**, *24* (47), 7467–7477.
        https://doi.org/10.1002/adfm.201401399.

(8)   Nguyen, K.; Bruce, B. D. Growing Green Electricity: Progress and Strategies for Use of
        Photosystem I for Sustainable Photovoltaic Energy Conversion. *Biochimica et Biophysica Acta
        (BBA) - Bioenergetics* **2014**, *1837* (9), 1553–1566.
        https://doi.org/10.1016/j.bbabio.2013.12.013.

(9)   Freestone, I.; Meeks, N.; Sax, M.; Higgitt, C. The Lycurgus Cup — A Roman Nanotechnology.
        Gold Bull **2007**, *40* (4), 270–277. https://doi.org/10.1007/BF03215599.

(10)   Qiu, Y.; Liu, Y.; Wang, L.; Xu, L.; Bai, R.; Ji, Y.; Wu, X.; Zhao, Y.; Li, Y.; Chen, C. Surface Chemistry
        and Aspect Ratio Mediated Cellular Uptake of Au Nanorods. *Biomaterials* **2010**, *31* (30), 7606–
        7619. https://doi.org/10.1016/j.biomaterials.2010.06.051.

(11)   Bharadwaj, P.; Novotny, L. Spectral Dependence of Single Molecule Fluorescence
        Enhancement. *Opt. Express* **2007**, *15* (21), 14266–14274.
        https://doi.org/10.1364/OE.15.014266.

(12)   Masson, J.-F. Surface Plasmon Resonance Clinical Biosensors for Medical Diagnostics. *ACS
        Sens.* **2017**, *2* (1), 16–30. https://doi.org/10.1021/acssensors.6b00763.

(13)   Liang, Z.; Sun, J.; Jiang, Y.; Jiang, L.; Chen, X. Plasmonic Enhanced Optoelectronic Devices.
        Plasmonics **2014**, *9* (4), 859–866. https://doi.org/10.1007/s11468-014-9682-7.

(14)   Friebe, V. M.; Delgado, J. D.; Swainsbury, D. J. K.; Gruber, J. M.; Chanaewa, A.; van Grondelle,
        R.; von Hauff, E.; Millo, D.; Jones, M. R.; Frese, R. N. Plasmon-Enhanced Photocurrent of
        Photosynthetic Pigment Proteins on Nanoporous Silver. *Advanced Functional Materials* **2016**,
        26 (2), 285–292. https://doi.org/10.1002/adfm.201504020.

(15)   Sun, Y.; Yin, Y.; Mayers, B. T.; Herricks, T.; Xia, Y. Uniform Silver Nanowires Synthesis by
        Reducing AgNO3 with Ethylene Glycol in the Presence of Seeds and Poly(Vinyl Pyrrolidone).
        Chemistry of Materials **2002**, *14* (11), 4736–4745.

(16)   Kondo, M.; Iida, K.; Dewa, T.; Tanaka, H.; Ogawa, T.; Nagashima, S.; Nagashima, K. V. P.;
        Shimada, K.; Hashimoto, H.; Gardiner, A. T.; et al. Photocurrent and Electronic Activities of
        Oriented-His-Tagged Photosynthetic Light-Harvesting/Reaction Center Core Complexes
        Assembled onto a Gold Electrode. *Biomacromolecules* **2012**, *13* (2), 432–438.
        https://doi.org/10.1021/bm201457s.

(17)   Ataka, K.; Giess, F.; Knoll, W.; Naumann, R.; Haber-Pohlmeier, S.; Richter, B.; Heberle, J.
        Oriented Attachment and Membrane Reconstitution of His-Tagged Cytochrome c Oxidase to a

Gold Electrode: In Situ Monitoring by Surface-Enhanced Infrared Absorption Spectroscopy. *J. Am. Chem. Soc.* **2004**, *126* (49), 16199–16206. https://doi.org/10.1021/ja045951h.

(18) Badura, A.; Esper, B.; Ataka, K.; Grunwald, C.; Wöll, C.; Kuhlmann, J.; Heberle, J.; Rögner, M. Light-Driven Water Splitting for (Bio-)Hydrogen Production: Photosystem 2 as the Central Part of a Bioelectrochemical Device. *Photochemistry and Photobiology* **2006**, *82* (5), 1385–1390. https://doi.org/10.1562/2006-07-14-RC-969.

(19) Haxo, F. T.; Kycia, J. H.; Somers, G. F.; Bennett, A.; Siegelman, H. W. Peridinin-Chlorophyll a Proteins of the Dinoflagellate Amphidinium Carterae (Plymouth 450) 1. *Plant Physiol.* **1976**, *57* (2), 297–303.

(20) Hofmann, E.; Wrench, P. M.; Sharples, F. P.; Hiller, R. G.; Welte, W.; Diederichs, K. Structural Basis of Light Harvesting by Carotenoids: Peridinin-Chlorophyll-Protein from Amphidinium Carterae. *Science* **1996**, *272* (5269), 1788–1791. https://doi.org/10.1126/science.272.5269.1788.

(21) Olejnik, M.; Krajnik, B.; Kowalska, D.; Twardowska, M.; Czechowski, N.; Hofmann, E.; Mackowski, S. Imaging of Fluorescence Enhancement in Photosynthetic Complexes Coupled to Silver Nanowires. *Applied Physics Letters* **2013**, *102* (8), 083703-083703–083705. https://doi.org/doi:10.1063/1.4794171.

(22) Czechowski, N.; Nyga, P.; Schmidt, M.; Brotosudarmo, T.; Scheer, H.; Piatkowski, D.; Mackowski, S. Absorption Enhancement in Peridinin–Chlorophyll–Protein Light-Harvesting Complexes Coupled to Semicontinuous Silver Film. *Plasmonics* **2012**, *7* (1), 115–121. https://doi.org/10.1007/s11468-011-9283-7.

(23) Olejnik, M. Unpublished.

(24) Haniewicz, P.; Abram, M.; Nosek, L.; Kirkpatrick, J.; El-Mohsnawy, E.; Olmos, J. D. J.; Kouřil, R.; Kargul, J. M. Molecular Mechanisms of Photoadaptation of Photosystem I Supercomplex from an Evolutionary Cyanobacterial/Algal Intermediate. *Plant Physiology* **2018**, *176* (2), 1433–1451. https://doi.org/10.1104/pp.17.01022.

(25) Kargul, J.; Janna Olmos, J. D.; Krupnik, T. Structure and Function of Photosystem I and Its Application in Biomimetic Solar-to-Fuel Systems. *J. Plant Physiol.* **2012**, *169* (16), 1639–1653. https://doi.org/10.1016/j.jplph.2012.05.018.

(26) Kowalska, D.; Steer, R. P. Quenching of MgTPP and ZnTPP Fluorescence by Molecular Oxygen. *Journal of Photochemistry and Photobiology A: Chemistry* **2008**, *195* (2), 223–227. https://doi.org/10.1016/j.jphotochem.2007.10.011.

(27) Tripathy, U.; Kowalska, D.; Liu, X.; Velate, S.; Steer, R. P. Photophysics of Soret-Excited Tetrapyrroles in Solution. I. Metalloporphyrins: MgTPP, ZnTPP, and CdTPP. *J. Phys. Chem. A* **2008**, *112* (26), 5824–5833. https://doi.org/10.1021/jp801395h.

(28) Kowalska, D.; Liu, X.; Tripathy, U.; Mahammed, A.; Gross, Z.; Hirayama, S.; Steer, R. P. Ground- and Excited-State Dynamics of Aluminum and Gallium Corroles. *Inorg. Chem.* **2009**, *48* (6), 2670–2676. https://doi.org/10.1021/ic900056n.

(29) Kowalska, D.; Haro-González, P.; Martín, I. R.; Cáceres, J. M. Analysis of the Optical Properties of Er3+-Doped Strontium Barium Niobate Nanocrystals Using Time-Resolved Laser Spectroscopy. *Appl. Phys. A* **2010**, *99* (4), 771–776. https://doi.org/10.1007/s00339-010-5716-y.

(30) Haro-González, P.; Martín, I. R.; Martín, L. L.; Kowalska, D.; Cáceres, J. M. Crystallization Effect on Tm3+–Yb3+ Codoped SBN Glass Ceramics. *Optical Materials* **2010**, *32* (10), 1385–1388. https://doi.org/10.1016/j.optmat.2010.03.014.

(31) Olejnik, M.; Krajnik, B.; Kowalska, D.; Lin, G.; Mackowski, S. Spectroscopic Studies of Plasmon Coupling between Photosynthetic Complexes and Metallic Quantum Dots. *J. Phys.: Condens. Matter* **2013**, *25* (19), 194103. https://doi.org/10.1088/0953-8984/25/19/194103.

(32) Szalkowski, M.; Ashraf, K. U.; Lokstein, H.; Mackowski, S.; Cogdell, R. J.; Kowalska, D. Silver Island Film Substrates for Ultrasensitive Fluorescence Detection of (Bio)Molecules. *Photosyn. Res.* **2016**, *127* (1), 103–108. https://doi.org/10.1007/s11120-015-0178-x.

(33) Maćkowski, S.; Czechowski, N.; Ashraf, K. U.; Szalkowski, M.; Lokstein, H.; Cogdell, R. J.; Kowalska, D. Origin of Bimodal Fluorescence Enhancement Factors of Chlorobaculum Tepidum Reaction Centers on Silver Island Films. *FEBS Lett* **2016**, *590* (16), 2558–2565. https://doi.org/10.1002/1873-3468.12292.

(34) Czechowski, N.; Lokstein, H.; Kowalska, D.; Ashraf, K.; Cogdell, R. J.; Mackowski, S. Large Plasmonic Fluorescence Enhancement of Cyanobacterial Photosystem I Coupled to Silver Island Films. *Applied Physics Letters* **2014**, *105* (4), 043701. https://doi.org/10.1063/1.4891856.

(35) Prymaczek, A.; Cwierzona, M.; Grzelak, J.; Kowalska, D.; Nyk, M.; Mackowski, S.; Piatkowski, D. Remote Activation and Detection of Up-Converted Luminescence *via* Surface Plasmon Polaritons Propagating in a Silver Nanowire. *Nanoscale* **2018**, *10* (26), 12841–12847. https://doi.org/10.1039/C8NR04517H.

(36) Nazir, R.; Balčiūnas, E.; Buczyńska, D.; Bourquard, F.; Kowalska, D.; Gray, D.; Maćkowski, S.; Farsari, M.; Gryko, D. T. Donor–Acceptor Type Thioxanthones: Synthesis, Optical Properties, and Two-Photon Induced Polymerization. *Macromolecules* **2015**, *48* (8), 2466–2472. https://doi.org/10.1021/acs.macromol.5b00336.

(37) Klemens, T.; Świtlicka-Olszewska, A.; Machura, B.; Grucela, M.; Janeczek, H.; Schab-Balcerzak, E.; Szlapa, A.; Kula, S.; Krompiec, S.; Smolarek, K.; et al. Synthesis, Photophysical Properties and Application in Organic Light Emitting Devices of Rhenium(I) Carbonyls Incorporating Functionalized 2,2':6',2''-Terpyridines. *RSC Adv.* **2016**, *6* (61), 56335–56352. https://doi.org/10.1039/C6RA08981J.

(38) Kiliszek, M.; Harputlu, E.; Szalkowski, M.; Kowalska, D.; Unlu, C. G.; Haniewicz, P.; Abram, M.; Wiwatowski, K.; Niedziółka-Jönsson, J.; Maćkowski, S.; et al. Orientation of Photosystem I on Graphene through Cytochrome C553 Leads to Improvement in Photocurrent Generation. *Journal of Materials Chemistry A* **2018**, *6* (38), 18615–18626. https://doi.org/10.1039/C8TA02420K.

Dorota Kowalska